

Quantification of progression and regression of carotid vessel atherosclerosis using 3D ultrasound images

Bernard Chiu, Micaela Egger, J. David Spence, Grace Parraga and Aaron Fenster

Abstract—Atherosclerosis is an inflammatory process similar to scar formation in the inner wall of the artery. It is the underlying cause of heart attacks and some strokes. Atherosclerotic lesions in the artery wall are called plaques. 3D ultrasound (US) has been used to monitor the progression of carotid vessel plaques in symptomatic and asymptomatic patients. Different ways of measuring various ultrasound phenotypes of atherosclerosis have been developed. Here, we report on the development and application of a method used to analyze changes in carotid plaque morphology from 3D US. In an effort to extend our previous work in plaque thickness analysis, we developed a procedure that facilitates the visualization and comparison of the distribution of plaque thickness by mapping the 3D arterial structure into a 2D plane.

I. INTRODUCTION

Atherosclerosis is a disease that encompasses the plaque build up process in the arterial wall, which ultimately leads to myocardial infarction and some strokes. The 3D US imaging approach developed by Fenster et al. [1], [2] has been used to image patients' carotid arteries and measure carotid atherosclerotic burden [9]. These measurements may aid in the management and monitoring of patients [3], and in evaluating the effect of new treatment options [5]. Different ultrasound phenotypes of atherosclerosis have been assessed, such as carotid stenosis severity [6], intima-media thickness [7], plaque composition [8] and volume [5],[9],[10]. Although these metrics assist in

Manuscript received March 31, 2006. This work was supported in part by Canadian Institute of Health Research and the Ontario R & D Challenge Fund. A.F. holds a Canada Research Chair in Biomedical Engineering, and acknowledges the support of the Canada Research Chair Program. B.C. acknowledges the support by the Ontario Graduate Scholarship. Both B.C. and M.E. acknowledge the support of the CIHR Strategic Training Program in Vascular Research.

B.C. is with the Imaging Research Laboratories, Robarts Research Institute, London, Ontario, Canada and is a PhD graduate student in the Graduate Program in Biomedical Engineering at The University of Western Ontario (e-mail: bchiu@imaging.robarts.ca).

M.E. is with the Imaging Research Laboratories, Robarts Research Institute, London, Ontario, Canada and is a MSc graduate student in the Department of Medical Biophysics at The University of Western Ontario (email: megger@imaging.robarts.ca).

J.D.S. is with the director of the Stroke Prevention & Atherosclerosis Research Centre, Robarts Research Institute, London, Ontario, Canada (email: dspence@robarts.ca).

G.P. is with the Imaging Research Laboratories, Robarts Research Institute, London, Ontario, Canada (email: gep@imaging.robarts.ca).

A.F. is the director of the Imaging Research Laboratories, Robarts Research Institute, London, Ontario N6A 5K8, Canada (e-mail: afenster@imaging.robarts.ca).

the management of carotid atherosclerosis, single-valued measurements do not provide sufficient information on the spatial distribution of plaques changes and burden in the carotid vessels. This information could improve our understanding of plaque progression and regression in response to therapy.

The spatial distribution of arterial narrowing (stenosis) was studied by Barratt et al. [10] and Yao et al. [11]. Both researchers quantified the degree of stenosis by determining the ratio between the diameter (or area) of the lumen and the wall on each cross-sectional slice of the vessel. Both the diameter or area ratio thus calculated can be plotted as a function of the length along the vessel. Although such stenosis profiles are useful in describing the distribution of plaque along the vessel, it is a single-valued measurement for each slice. Although the stenosis profile indicates the exact slices in which plaque burden was located, it gave no information as to where the plaque burden was located within a slice. Furthermore, because of compensatory enlargement, plaque itself does not necessarily cause stenosis [12].

We reported [13] on the development of a localized metric to quantify the plaque thickness change on a point-by-point basis. In this study, two 3D ultrasound images were obtained from each patient at two time points. The wall and the lumen were then manually segmented from each US image, and then we performed statistical tests to determine whether the thickness change was statistically significant. For a patient who had undergone three months of high-dose (80mg) atorvastatin treatment, we demonstrated that the carotid plaque had regressed significantly. This result agrees with the plaque volume comparison study performed for the same patient [5].

While overlaying the thickness map on the 3D carotid vessel wall (see Fig. 4 and 5) gives important information on the spatial distribution of plaque, comparison of different 3D thickness maps is difficult due to the anatomical variability of the vessels scanned at different time points. A solution of this problem is to flatten the carotid vessel based on some objective criteria. The goal of this paper is to develop a mapping scheme to flatten the carotid vessel, when provided a meshed surface representing the vessel wall.

II. METHODS

The problem of surface flattening from 3D into 2D space has been tackled by many investigators in the context of

map-making for the earth [14]. Gauss proved that surface flattening involves distortions either in angles or areas unless the surface has zero Gaussian curvature [15]. Many surface flattening methods have been proposed to minimize these distortions in some sense, and [16] provides a good review of these methods. In this paper, we introduce a method that preserves the arc length of each 2D average contour. Since the motivation of this work was to flatten a 3D carotid vessel thickness map, we also introduce how the thickness map was constructed in the next two sections.

A. Computation of Average Contours and Surfaces

The surface meshes representing five segmentations of the arterial wall were re-sliced by a 2D plane, resulting in five 2D contours as shown in Fig. 1 [13]. A line with direction determined by the correspondence relationship of the curves [13] intersected the manually segmented contours, resulting in five intersections, for which the centroid was computed. This process is performed in each vertex of the curves and the average contour is the curve containing all the centroids thus computed.

The manually segmented meshes were re-sliced with a stack of slices 1mm apart and the average contour in each slice was computed. The average contours on all 2D slices were then reconstructed to form a surface [13].

B. Computation of the thickness map

A stack of parallel transverse planes was used to slice the average surfaces of the arterial wall and lumen at 1mm interval. The distance between the average carotid vessel wall and lumen contours was computed and superimposed on the surface of the vessel wall. This distance measure incorporates the thickness of the intima and media of the vessel in addition to the atherosclerotic plaque thickness, since the arterial wall segmentation was performed for the adventitia-wall interface.

C. Construction of the Flattened Map

1) Common Carotid Artery (CCA)

We cut the carotid artery in the orientation shown in Fig. 2. The orientation of the plane cutting the CCA was determined by the following steps: (1) the centroids of the ICA and ECA slices immediately distal to the bifurcation apex (C_{ICA} and C_{ECA}) were computed and joined together by a line, which intersects the ICA and ECA slices at I_i and I_e respectively (see Fig. 2); (2) the tangents of both the ICA slice at I_i and the ECA slice at I_e were computed and the average direction of these two tangents was obtained; and, (3) the cutting plane was defined to be the plane containing the midpoint of I_i and I_e with normal defined by $N_T \times T$, where N_T is the normal of the transverse slice on which 2D average contours were obtained and T is the vector parallel to the tangent determined in step 2 (see Fig. 2).

The tangent line defined in step 2 above cut the CCA at two points, I_{c1} and I_{c2} . Starting from I_{c2} , the CCA contour,

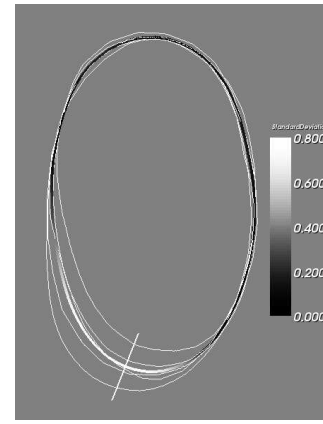


Fig. 1. Manually segmented contours (in white) obtained by re-slicing the carotid arterial wall surface and the average contours with standard deviation colour-coded and mapped on top to represent the intra-observer variability. A line approximately normal to the manually segmented contours intersected the segmented boundaries, resulting in five intersections for which average and standard deviation were computed.

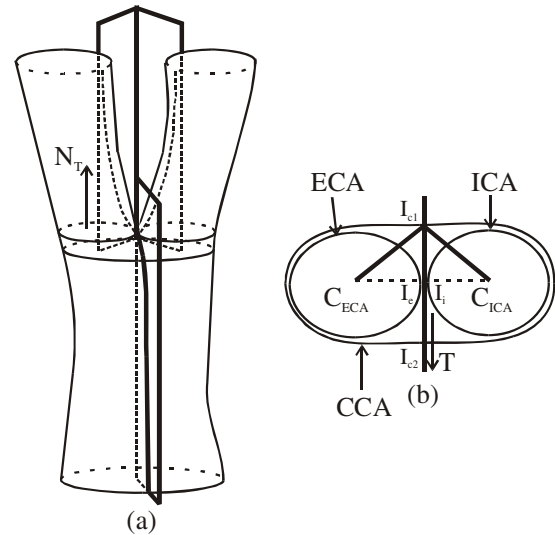


Fig. 2. (a) The front view and (b) the bird-eye view showing the orientation of the cutting planes that cut the common, external and internal carotid arteries

parameterized by arc length, was mapped into a straight line with the vertical coordinate (y) equalling to the distance between the bifurcation apex and the plane containing the contour. The point I_{c1} was used as a reference point and mapped to $x = 0$ (see Fig. 3). This procedure was repeated for all average contours of the CCA obtained as described in Section A. The distance between the contiguous lines on the 2D flattened map is 1mm, which is the same as the distance between adjacent contours in the 3D map. We are aware that this mapping scheme does not necessarily preserve the vertical distance. For example, the distance between two I_{c1} points associated with contiguous slices does not equal 1mm unless the displacement between the two points is in the direction of N_T , the normal of the transverse plane containing 2D contours and this stringent requirement is only satisfied by a regular cylinder. However, the carotid vessel wall has a tubular topology in which 2D contours

lying on adjacent slices do not differ significantly in shape, position and circumference. Considering the tubular topology of the vessel and that the arc length for each slice is preserved in the mapping technique, the area distortion is minimal. The plaque volume can be approximated directly from the 2D flattened map by integrating the thickness in a diseased region. Landry et al. [17] found that the variance in the total plaque measurement is dominated by the variance in the identification of the plaque edges. The advantage of calculating the volume directly from the 2D flattened map is that a diseased region can be studied in detail by observing the map, before computing the volume. Thus, the use of the 2D flattened map may help in reducing the variance in plaque volume measurements.

2) Internal and External Carotid Artery (ICA and ECA)

Apart from minimizing area distortion, another criterion considered in our design of the mapping scheme is continuity. To facilitate the interpretation of the thickness map, it is desired that the mapping be continuous from the CCA to both the ICA and ECA. This involves defining proper correspondence relationships between the CCA slice immediately proximal to the bifurcation apex and both the ICA and ECA slices immediately distal to the apex. We defined the correspondence of I_{c1} (Fig. 3(a)) to be p_e , the intersection between the line drawn from C_{ECA} to I_{c1} and the ECA boundary. This correspondence relationship defines the cutting plane for the ECA (see Figs. 2 and 3(a)). The ECA contour, parameterized by arc length, was mapped into a straight line starting from p_e , which was mapped to the origin of the 2D map (Fig. 3(b)), in the counter-clockwise direction. The straight lines corresponding to the ECA contours were mapped to the negative-x half of the 2D plane, to match the parameterization used in mapping the CCA contours (Fig. 3(b)). The mapping was repeated for each average ECA contour.

A similar scheme was used in mapping the ICA contour, which was mapped in the clockwise direction starting from the intersection p_i (Fig. 3(a)). The ICA contours were mapped to the positive-x half of the 2D plane (Fig. 3(b)).

III. RESULTS

The thickness map computed for the patient who underwent atorvastatin treatment [5] was mapped into a 2D plane in order to evaluate the performance of the proposed mapping technique. The 3D US images were acquired at baseline and 3 months later for this patient, who received 80mg of atorvastatin daily during the interval between the two scanning sessions. The statin therapy has been shown to halt the progression or reduce the size of the atherosclerotic plaque [5].

The 3D US images were acquired by translating the ultrasound transducer (L12-5, 50mm, Philips, Bothel Washington) along the neck of the patient while video frames from an US machine (ATL HDI 5000, Philips, Bothel Washington) were digitized and saved to a computer

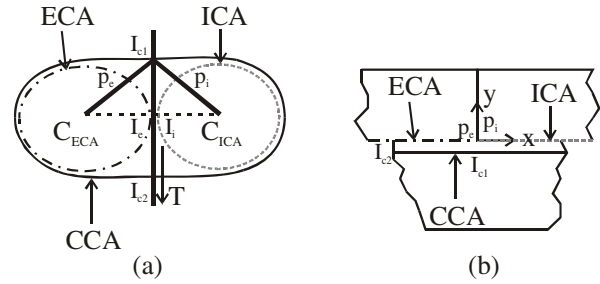


Fig. 3. The 2D mapping specifications: (a) The CCA contour immediately proximal to the bifurcation apex (solid line), the ECA (—●—) and ICA (-----) immediately distal to the apex and (b) their correspondence in the 2D flattened map

workstation. The resulting transverse 2D images were parallel to each other with a mean spatial interval of 0.15 mm. The acquired 2D images were reconstructed to form a 3D US image, which was displayed using a 3D viewing software [5],[13].

Fig. 4 and 5 show the 2D and 3D thickness maps for the patient at baseline and three months later respectively. We observed from Fig. 4 (a) and (b) that there was a 9-mm thick diseased region located on the side of the CCA extending into the ICA. This region was continuously mapped to the 2D flattened map (Fig. 4(c)) as expected. Similar comment applies to the maps in Fig. 5. We do not observe a significant area distortion in the mapping technique, although quantitative measurements should be obtained to verify this qualitative assessment in our future work.

We observed that there was significant plaque regression in the CCA by comparing the 2D flattened maps shown in Fig. 4(c) and 5(c). To confirm this qualitative assessment, we flattened the thickness change map obtained and compared the resulting 2D map with those in Fig. 4(c) and 5(c). The plaque regression region can be clearly visualized and quantified in the 2D map shown in Fig. 6(c).

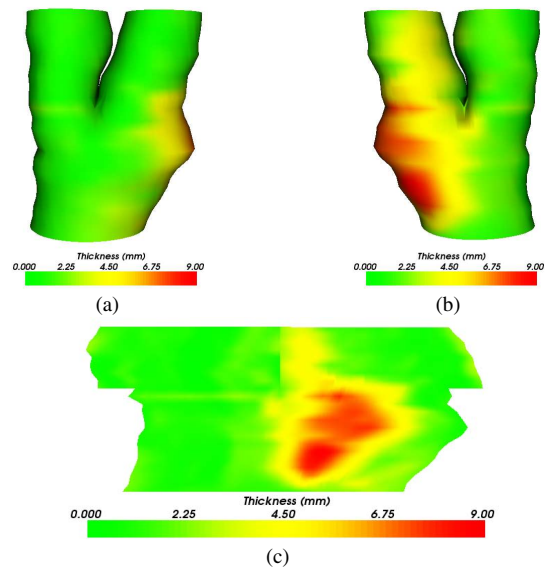


Fig. 4. (a) Front and (b) back view of the thickness map computed for the 3D US image acquired at baseline and (c) its correspondent flattened map. The front view is the view as displayed in Fig. 2(a).

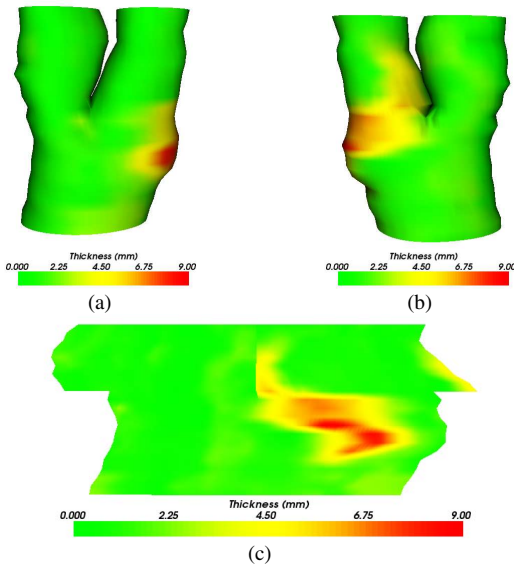


Fig. 5. (a) Front and (b) back view of the thickness map computed for the 3D US image acquired at three months after the Atorvastatin treatment had been initiated, and (c) the corresponding flattened map

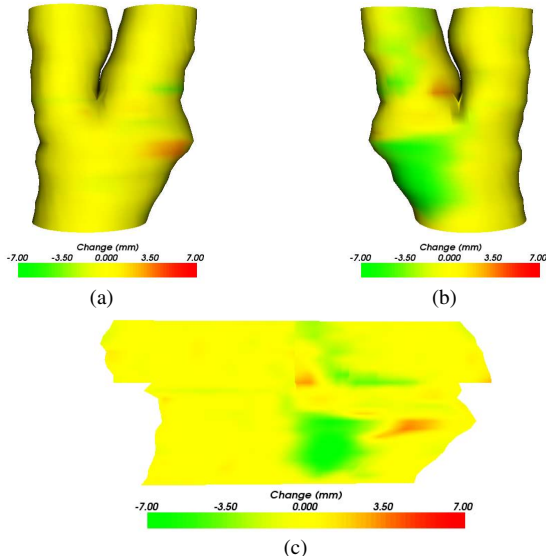


Fig. 6. (a) Front and (b) back view of the thickness change map computed using the method described in [13] and (c) its corresponding thickness map

IV. CONCLUSIONS

Anatomical variability exists in a patient's carotid vessel scanned at different time points, which renders the comparison between the 3D (plaque + intima-media) thickness maps to be difficult. We described a technique that allows an objective comparison between the thickness maps obtained at two different time points.

This approach may be used to evaluate the location of plaque progression and regression in relation to localized disturbances of flow patterns, such as oscillatory shear [18].

We considered two important criteria in designing the mapping scheme: (a) minimizing the area distortion, and (b) the continuity of the flattened map on both the CCA to ICA

and CCA to ECA borders. In our study of the thickness change in a patient under atorvastatin treatment, there was no significant distortion in our mapping technique and we showed that the diseased region on the CCA extending to the ICA was continuously mapped to the 2D flattened map.

REFERENCES

- [1] A. Fenster, D. B. Downey and H. N. Cardinal, "Topical review: Three-dimensional ultrasound imaging," *Phys. Med. Biol.*, vol. 46, R67-R99, 2001.
- [2] S. Tong, D. B. Downey, H. N. Cardinal, and A. Fenster, "Three-dimensional ultrasound prostate imaging system," *Ultrasound Med. Biol.*, vol. 22, pp.735-746, 1996.
- [3] J.D. Spence, M. Eliasziw, M. DiCicco, D.G. Hackam, R. Galil and T. Lohmann, "Carotid plaque area: a tool for targeting and evaluating vascular preventive therapy," *Stroke*, vol. 33, pp.2916-2922, 2002.
- [4] D.G. Hackam, J.C. Peterson and J.D. Spence, "What level of plasma homocyst(e)ine should be treated? Effects of vitamin therapy on progression of carotid atherosclerosis in patients with homocyst(e)ine levels above and below 14 mmol/L," *Am. J. Hypertens.*, vol. 13, pp.105-110, 2000.
- [5] C.D. Ainsworth, C.C. Blake, A. Tamayo et al. "3-Dimensional ultrasound measurement of change in carotid plaque volume: A tool for rapid evaluation of new therapies," *Stroke*, Vol. 36, no. 9, pp. 1904-1909, 2005.
- [6] C. Liapis, J. Kakisis, V. Papavassiliou et al., "Internal carotid artery stenosis: rate of progression," *Eur. J. Vasc. Endovasc. Surg.*, vol. 19(2), pp.111-117, 2002.
- [7] R.A., Markus, W.J. Mack, S.P. Azen and H.N. Hodis, "Influence of lifestyle modification on atherosclerotic progression determined by ultrasonographic change in the common carotid intima-media thickness," *Am. J. Clin. Nutr.*, vol. 65(4), pp. 1000-1004, 1997.
- [8] J.M. Seeger, E. Barratt, G. Lawson and N. Klingman, "The relationship between carotid plaque composition, plaque morphology and neurologic symptoms," *J. Surg. Res.*, vol. 58(3), pp. 330-336.
- [9] A. Landry, J.D. Spence and A. Fenster, "Measurement of carotid plaque volume by 3-dimensional ultrasound," *Stroke*, vol. 35(4), pp.864-869, 2004.
- [10] D.C. Barratt, B.B. Ariff, K.N. Humphries et al., "Reconstruction and quantification of the carotid artery bifurcation from 3D ultrasound images," *IEEE Trans. Medical Imaging*, vol. 23(5), pp. 567-583, 2004.
- [11] J. Yao, M.R.H.M. van Sambeek, A. D. Agata et al., "Three-dimensional ultrasound study of carotid arteries before and after endarterectomy," *Stroke*, vol. 29, pp.2026-2031, 1998.
- [12] S. Glagov, E. Weisenberg, C.K. Zarins, R. Stankunavicius, G.J. Kolettis, "Compensatory enlargement of human atherosclerotic coronary arteries," *N Engl J Med*. Vol. 316(22), pp. 1371-1375, 1987.
- [13] B. Chiu, M. Egger, J.D. Spence, G. Parraga and A. Fenster, "Quantification of carotid vessel atherosclerosis," *Proceedings of the SPIE International Symposium on Medical Imaging 2006*, February 11-16, 2006.
- [14] J.P. Snyder, *Flattening the earth: Two thousand years of map projections*, The Univ. of Chicago Press, 1993.
- [15] M.P. Do Carmo, *Differential geometry of curves and surfaces*, Prentice-Hall, 1976.
- [16] M. S. Floater and K. Hormann, Surface Parameterization: a Tutorial and Survey, in *Advances in Multiresolution for Geometric Modelling*, N. A. Dodgson, M. S. Floater, and M. A. Sabin (eds.), Springer-Verlag, Heidelberg, 2005, 157-186.
- [17] A. Landry, J.D. Spence and A. Fenster, "Quantification of carotid plaque volume measurements using 3D ultrasound imaging," *Ultrasound in Med. & Biol.*, Vol. 31(6), pp.751-762, 2005.
- [18] J.B. Thomas, J.S. Milner, B.K. Rutt and D.A. Steinman, "Reproducibility of image-based computational fluid dynamics models of the human carotid bifurcation," *Ann Biomed Eng.* Vol 31(2), pp. 132-141, 2003.